

# On the scalability of the operating capacity of hydrogen recombiners

Alexandr V. Avdeenkov<sup>1</sup>, Sergey G. Kalyakin<sup>1</sup>, Sergey L. Soloviev<sup>1</sup>, Huong Duong Quang<sup>2</sup>

<sup>1</sup> All-Russian Research Institute for Nuclear Power Plants Operation, Ferganskaya st., 25, Moscow, 109507, Russia

<sup>2</sup> Obninsk Institute for Nuclear Power Engineering, National Research Nuclear University MEPhI, Studgorodok, 1, Obninsk, Kaluga region, 249020, Russia

Corresponding author: Alexandr V. Avdeenkov (avavdeenkov@vniiaes.ru)

**Academic editor:** Georgy Tikhomirov ♦ **Received** 8 March 2022 ♦ **Accepted** 17 June 2022 ♦ **Published** 28 June 2022

**Citation:** Avdeenkov AV, Kalyakin SG, Soloviev SL, Duong Quang H (2022) On the scalability of the operating capacity of hydrogen recombiners. Nuclear Energy and Technology 8(2): 143–152. <https://doi.org/10.3897/nucet.8.83223>

## Abstract

One of the main factors in the capacity of passive autocatalytic recombiners (PARs) is its productivity or the hydrogen removal rate. In this work it was demonstrated that regardless of the type of a recombiner, the hydrogen removal rate is mostly determined by the catalytic surface area and the molar density of hydrogen at the inlet. It means that the performance of a recombiner should obey geometric and physical scalability.

Geometric scalability is characterized by the retention of the specific (per unit area of the catalytic surface) hydrogen removal rate with increasing the size of the recombiner by increasing the inlet section while maintaining the height and design of the catalytic unit.

Physical scalability is characterized by maintaining the hydrogen removal rate of the recombiner at a constant input molar density of hydrogen in an air-hydrogen environment while simultaneously changing the input temperature and pressure.

For a numerical demonstration of scalability, several calculations were performed with different initial hydrogen concentrations, external conditions and amounts of catalytic elements. It was shown that, regardless of the number of catalytic plates in the recombiner, the specific removal rate of hydrogen will remain unchanged and that under different external conditions (temperature, pressure), in case they correspond to the same inlet hydrogen density, the hydrogen removal rate does not change.

## Keywords

recombiner, scalability, chemical kinetics, hydrogen removal rate

## Introduction

The most common practice of removing hydrogen from the enclosure vessel (EV) of a nuclear plant is based on the principle of passive catalytic hydrogen recombination using catalytic elements containing some catalysts (Della Loggia 1992, Ferroni et al. 1994, International Atomic

Energy Agency 2001, Reinecke et al. 2010, Avdeenkov et al. 2018). The catalyst units are ceramics coated with thin (micrometer range) washcoats of catalysts like platinum (Pt) and palladium (Pd) (Klauck et al. 2014, Rozeń 2015a, Saint-Just and Etemad 2016, Arnould et al. 2021). The activity of these catalysts depends on their composition, structure, and intended application, and therefore

may vary. Catalytic elements are assembled into catalytic blocks and units, and can be of various geometric shapes, including sheets made of stainless steel and coated with Pt/Pd substrate catalyst material (Framatome 2022), and cylindrical catalytic elements made of ceramic with a Pt coating (Russkiye Energeticheskkiye Tekhnologii 2021).

The passive autocatalytic recombiner (PAR) has a standard design with a catalytic unit placed at the bottom of a rectangular steel tube (as a rule) with an open outlet. The exit part is blind from above, one or several side parts at the exit are covered with a metal mesh (lattice). When hydrogen appears in the internal volume of the recombiner, an exothermic reaction of hydrogen and oxygen recombination into water begins on the catalytic surface, which ensures the onset of natural convection. PAR does not require external power supply or any control.

Recombiners of the RVK line (Russkiye Energeticheskkiye Tekhnologii 2021) (manufactured by CJSC INPK RET, Russia) and the FR line (Framatome 2022) (manufactured by AREVA/Siemens) have been certified and used at Russian Nuclear Power Plants (NPPs). Fig. 1 shows a typical RVK-500 recombiner and Fig. 2 shows a FR90/1-1500 one. The basic principles of the PAR operation are the same, however, the catalysts used can differ significantly (there are some other commercial and implemented PARs with catalyst sheets from AECL, Canada, or PARs with porous catalyst beds from NIS, Germany, Arnould et al. 2021). The catalyst unit of an RVK type recombiner contains catalytic cylindrical rods while the AREVA recombiners contain plates. The number of rods or plates is different for different models and define the recombiner size and sometimes geometry. For example, RVK-500 contains 696 rods while RVK-1000 contains twice as many rods as RVK-500. The height of each rod

is 64 mm and the diameter is 5 mm. The number of catalytic sheets for FR90/1-1500 PAR is 150 which is twice larger than for FR 90/1-750 PAR. The size of each sheet is 140×290mm.

The full-scale validation of large recombiners is usually very difficult. Therefore, most experimental studies are carried out on recombiners such as RVK-500, RVK-1000, or on separate modules of large recombiners. The largest PAR of this line, RVK-4, consists of four identical modules. RVK-3 consists of two of the same modules (International Atomic Energy Agency 2001). The number of rods in one RVK-4 module is five times larger than in RVK-500.

One of the basic characteristics of a recombiner is its productivity (or hydrogen removal rate). The estimates show that the release of hydrogen during a severe accident at NPPs (like VVER-1000 and similar) can range up to several hundred kilograms per hour depending on the scenario of the accident, the type and size of the reactor. The productivity of recombiners is sometimes given in terms of the inlet area. PARs on the average show a hydrogen removal rate (at 4 vol% and a pressure of 1 bar) in the region of 3–7 kg per hour and per 1m<sup>2</sup> inlet section (International Atomic Energy Agency 2001, Passive Catalytic Hydrogen Recombiner 2004, 2005), which increases almost linearly with an increase in the hydrogen concentration at the inlet (usually up to 8 vol%) and an increase in pressure (with an increase in molar density). For projects of large pressurized water reactors, the total area of the inlet section of the recombiners can be up to several tens of square meters.

It should be noted that the performance characteristics of the recombiners declared by the manufacturers were frequently obtained for quite specific external conditions,

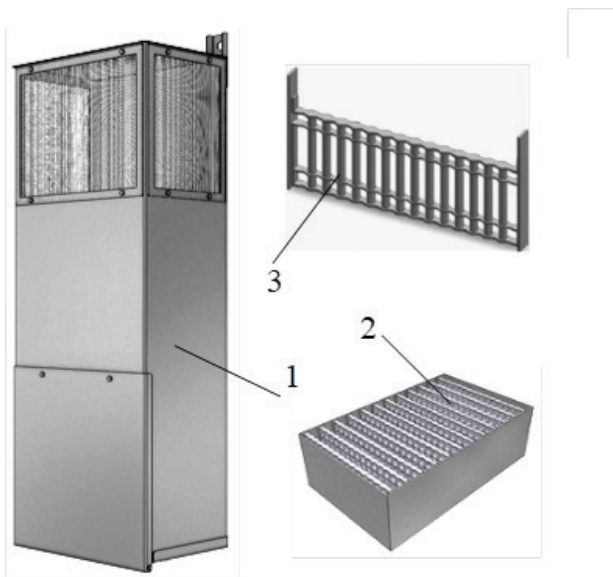


**Figure 1.** Picture of RVK-500 PAR, Russkiye Energeticheskkiye Tekhnologii 2021: 1- PAR framework, 2 – catalyst unit consisting of a set of catalytic frames, 3 – catalyst rods combined in frames.



**Figure 2.** Picture of FR90/1-1500, Framatome 2022. 1- PAR framework; 2 – catalyst unit; 3 – inlet; 4 – outlet; 5 – catalytic plates; A. Side view, unit extended; B. Bottom view.

namely in a quiescent environment in which the recombiner is self-starting in the natural circulation mode.

Under real conditions of a possible severe accident, the characteristics derived for such experimental conditions are hardly justified in being used for numerical simulation of the accident, since the characteristics of the recombiner essentially depend on the rate of hydrogen-air flow into the recombiner (Reinecke et al. 2005, Reinecke et al. 2010, Malakhov et al. 2020). Thus, the experimentally obtained properties provide only a certain general understanding of the recombiner hydrogen removal rate and its guiding technical characteristics.

For the RVK line of recombiners, the hydrogen removal rate was measured at an initial hydrogen concentration of less than 1% to over 11 vol.%. Based on the experimental data, empirical correlations for hydrogen removal rate have been derived in (Passive Catalytic Hydrogen Recombiner 2004, 2005) and verified in (Tarasov et al. 2017):

$$G(g/s)=n \times C \times [a_0 + a_1 \times (C-2) + a_2 \times (C-2)^2], \quad (1)$$

$$a_0 = 1.43 + 0.24 \times (P-1) + 0.005 \times (T-20),$$

$$a_1 = 0.12 + 0.0031 \times (P-1) + 0.0003 \times (T-20),$$

$$a_2 = 0.009 \times (P-1) + 1.08 \times 10^{-4} \times (T-20) - 1.54 \times 10^{-5} \times (T-20) \times (P-1),$$

$$n = 0.0077 \text{ for RVK-500,}$$

$$n = 0.0183 \text{ for RVK-1000,}$$

$$n = 0,16 \text{ for RVK-4,}$$

where  $C$  (vol.%) - the volume concentration of  $H_2$ ,  $P$  (bar) - pressure,  $T$  ( $^{\circ}C$ ) - temperature.

The resulting dependencies are purely empirical and we do not know if there are any verification calculations to justify the recombiner performance outside the experimental conditions.

The similar experimental approach to investigating the global behaviour of a recombiner in a larger environment has been performed for the AREVA type of recombiners. The derived empirical correlations (Bachelierie et al. 2003, Reinecke et al. 2010) describe the hydrogen removal rate for a reference PAR type as a function of the gas composition, temperature and pressure.

The empirical correlations (1) make it possible to determine the specific hydrogen removal rate of the catalytic elements (hydrogen removal rate per unit surface area of the catalyst). Fig. 3 shows the dependence of the specific hydrogen removal rate ( $G_s$ ) for two types of PAR, RVK and FR, as a function of the inlet volume concentration. The results of the comparison demonstrate that the specific hydrogen removal rates, taking into account possible errors in approximations, are fairly similar. This indicates that the absolute removal rate is mainly determined by the area of the catalytic surface, but only at low (<8 vol.%)

hydrogen concentrations. At higher hydrogen concentrations, the situation is not so unambiguous and may depend on the geometry of catalytic blocks.

The last statement can be justified as follows. At a low concentration the recombination takes place at catalyst surfaces and the area of those surfaces mostly determines the hydrogen removal rate while the geometry of catalytic elements (plates or rods and their relative positions) plays a minor role. At a higher concentration the recombination takes place both at catalyst surfaces and in gas phases in a recombiner volume and thus the geometry of a catalyst unit may define “the concentration of the ignition” of the air- hydrogen mixture.

It is reasonable to suggest that in case of severe accidents with a significant release of hydrogen, the environmental conditions around recombiners are not necessarily those for which the above correlations (Fig. 3) were obtained. It means that the empirical correlations similar to (1) have to be either improved or corrected for a broader variety of regimes especially with a different inlet velocity of a flow. In most cases, it is necessary to take into account the transient modes, since both the feed rate and the hydrogen concentration can change quite quickly, and the velocity of an air-hydrogen mixture entering the recombiner significantly affects its hydrogen removal rate. Thus, a full-scale numerical and even more experimental substantiation of the recombiner operation in all kinds of non-stationary and transient modes seems to be a difficult task, and the construction of a working model of a recombiner of any scale and for any environmental conditions is a necessary step to substantiating hydrogen safety.

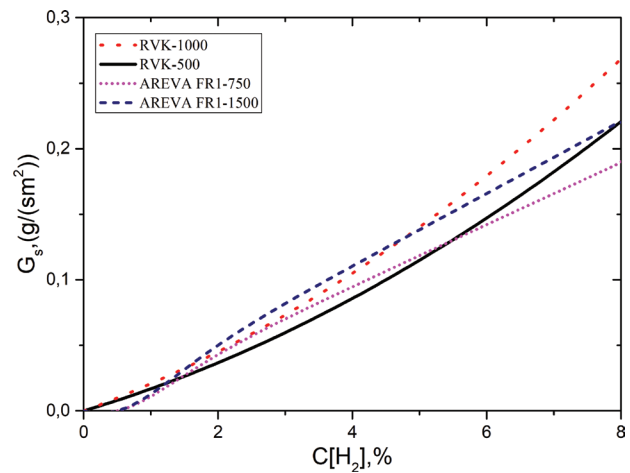


**Figure 3.** Comparison of the specific hydrogen removal rate of PARs of RVK and AREVA types, depending on the hydrogen volumetric concentration and based on the empirical correlations (1) for RVK recombiners and correlations (Bachelierie et al. 2003, Reinecke et al. 2010) for AREVA recombiners.

Regardless of the type of a recombiner, the hydrogen removal rate is mostly determined by the catalytic surface area and the mass density of hydrogen at the inlet. It means that the performance of a recombiner should obey geometrical and physical scalability.

To demonstrate such scalabilities for hydrogen removal rates, several calculations were performed with different initial hydrogen concentrations, external conditions and amounts of catalytic elements.

## Scalability for hydrogen removal rate

Here two types of a scalability are determined and considered that can be used to construct a realistic numerical model of the performance of recombiners.

Geometric scalability is characterized by the retention of the specific (per unit area of the catalytic surface) hydrogen removal rate while increasing the size of the recombiner by increasing the inlet section while maintaining the height and design of the catalytic unit. In this case, also, the hydrogen removal rate increases in proportion to the increase of the inlet section.

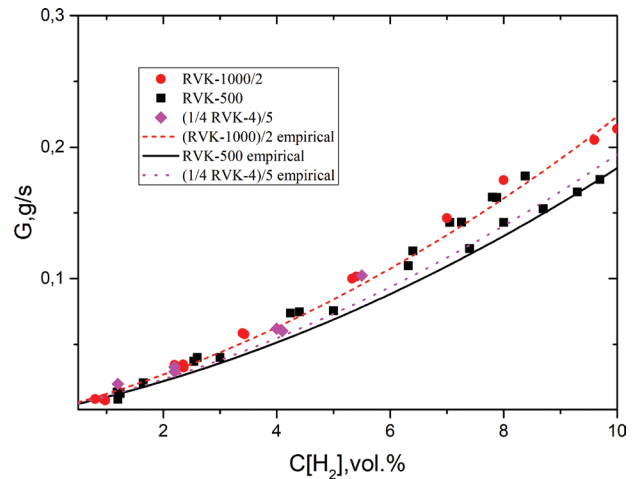
Physical scalability is characterized by the same hydrogen removal rate of the recombiner at the same inlet molar density of hydrogen with a simultaneous change in the inlet temperature and pressure. Here and below, we assume that the oxygen is in excess in the gas mixture for the hydrogen oxidation. In general, the “air” may contain water vapor and other gases.

Geometric scalability was rather closely investigated even in experimental works at Sandia National Laboratories on the Surtsey experimental setup (Blanchat and Malliakos 1999), which is an isolated vessel with an internal volume of 99 m<sup>3</sup>.

Three samples were used in the experiment: 1/2, 1/4, 1/8 of the full-scale prototype (size of the inlet section 1mx1m), consisting of two rows of 44 cartridges (1/2 – 44 (one row), 1/4 – 22, 1/8 – 11). Each cartridge is 0.45mx0.2mx0.01m in size. The scaling effect (proportional to the number of cartridges) was investigated in a mixture of 0.107Mpa of air and 0.107Mpa of steam. In the study, it was noted that “simple” forward scaling was only observed at low hydrogen concentrations; at high concentrations, a normalization factor was introduced to consider the incomplete mixing in the lower part of the setup and to take into account this heterogeneity in the model when processing the results.

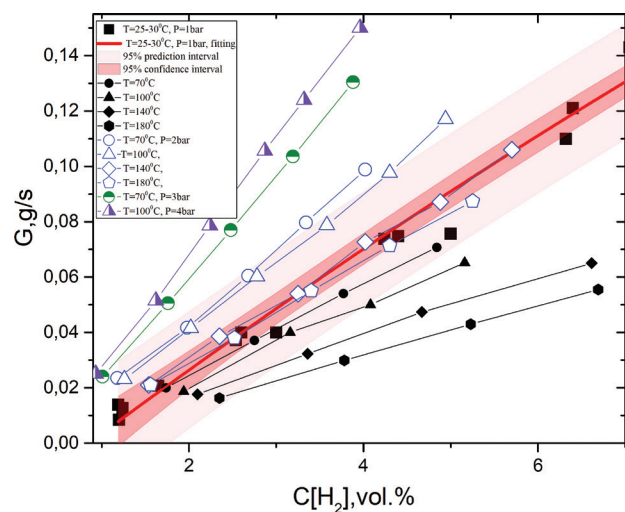
Experimental scaling studies of this kind were carried out with recombiners of the KPAR line (Jae-Won et al. 2011) having a honeycomb structure of a catalytic unit with a porous catalyst material. As an example, two samples have been considered, having the same height and differing in the area of the inlet section – the number of catalytic blocks by a factor of 4. The experiments were carried out with hydrogen concentrations in the range of about 2 – 8 vol.%. It has been demonstrated that the rate of hydrogen removal is proportional to the number of catalysts and does not depend on the size of the recombiner.

Fig. 4 shows some experimental data on hydrogen removal rates for the RVK-500 and RVK-1000 recombiners, divided by two, and one RVK-4 recombiner module (the recombiner consists of four identical modules), divided by



**Figure 4.** The experimental hydrogen removal rates (Passive Catalytic Hydrogen Recombiner 2004, 2005) in dependence on volumetric hydrogen concentration for different RVK recombiners under normal conditions ( $T=20-30$  °C,  $P=1$ bar). Empirical correlations (1) are used.

five. Such presentation of experimental data was chosen in order to make comparison of rates for cases with the same number of catalytic cylinders (or the same catalytic surfaces, see the introduction). This is the same as if we were comparing specific hydrogen removal rates for all these recombiners. The lines show the corresponding accepted empirical dependencies (1) derived in (Passive Catalytic Hydrogen Recombiner 2004, 2005) with the use of available experimental data (Passive Catalytic Hydrogen Recombiner 2004, 2005). Fig. 5 shows the experimental data for hydrogen removal rates in dependence on the inlet hydrogen concentration under normal conditions and conditions different from normal. Besides, Fig. 5 shows the fitting dependences and the corresponding 95% confidence and 95% prediction intervals for the experimental data obtained under normal conditions for the RVK-500 (black squares).



**Figure 5.** The experimental hydrogen removal rates (Passive Catalytic Hydrogen Recombiner 2004, 2005) in dependence on the volumetric hydrogen concentration for RVK-500 recombiner under normal conditions and conditions different from normal.

The fitted curves clearly demonstrate an almost linear dependence of the hydrogen removal rates on the volumetric hydrogen concentration. Possible deviations from the linear relationship (prediction interval) range from about 20% for RVK-500 to less than 10% for RVK-1000. The fitted curve for the RVK-4 is between the curves for the RVK-500 and RVK-1000 with the possible deviation close to 10%. The data presented in Fig. 4 demonstrate a clear geometrical scalability of a hydrogen removal rate within a 20% deviation which is the prediction interval considered above.

Fig. 5 shows the same dependencies as in Fig. 4, as well as empirical relationships for external conditions other than normal. The figure shows that the hydrogen removal rate is radically different under different external conditions for a given volumetric hydrogen concentration. Most of the data presented were obtained on a flow bench (Passive Catalytic Hydrogen Recombiner 2004, 2005) where the absolute pressure was measured. Thus, it is not clear if it was a fully natural circulation or somewhat of a forced circulation. In any case a greater pressure provides a higher hydrogen removal rate of the recombiners. At the same time, a higher speed of the mixture provides a higher hydrogen removal rate of the recombiners. This was also noted for plate catalysts (Reinecke et al. 2010).

The physical scalability is a direct consequence of the fact that we can treat our system as the mixture of ideal gases. Using the equation of state it is easy to derive that the inlet hydrogen molar density  $C_M = PC/(RT)$ , where  $P$  is the pressure,  $T$  is the temperature,  $R$  is the gas constant and  $C$  is the volumetric hydrogen concentration at inlet. It means that  $C_M$  is defined by the  $(P/T)$  ratio at fixed  $C$ .

Fig. 6 shows some of the same data as in Fig. 5 but recalculated in dependence on the molar concentration of hydrogen for the fixed volumetric hydrogen concentration. For example, the red circles are for the next  $P$ (in bar) and  $T$  (in °C) data: (4,100); (3,70); (2,70); (2,140) and (1,100) and the volumetric concentration is close to 4%

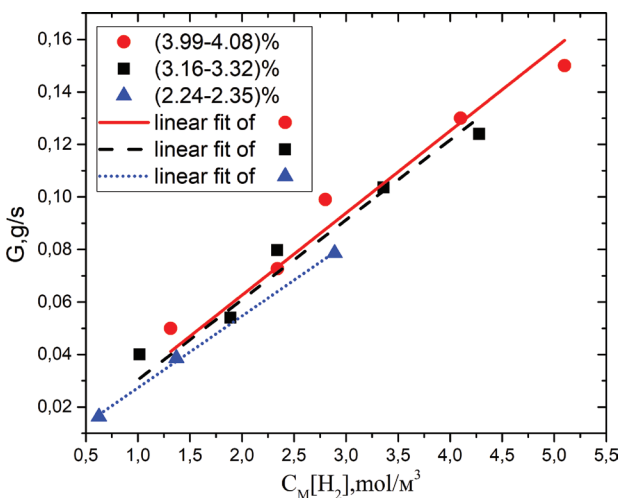


**Figure 6.** The experimental hydrogen removal rates (Passive Catalytic Hydrogen Recombiner 2004, 2005) in dependence on the hydrogen molar density for RVK-500 recombiner for some fixed values of volumetric hydrogen concentration.

for all points (it is not possible to choose the experimental data with exactly for 4vol.% hydrogen concentration). The linear fit follows  $G=0.0313C_M$  or  $G \approx 1.5e-4(P/T)$  dependency with about 15% of maximal deviation. It means that we can calculate the hydrogen removal rate at any inlet  $(P, T)$  set which provides the chosen 4vol%. The same consideration works for other inlet volumetric hydrogen concentrations but with other linear fits (Fig.6).

Moreover, we found that the physical scalability may work even in a broader way. If some sets of data for  $P$  (in bar),  $T$ (in °C) and  $C$  (in%) provide rather similar values of  $C_M$  then it is expected to have a very similar hydrogen removal rate as well. For example, sets of  $(P, T, C)$  with (3, 70, 4) and (4, 100, 3.32) provide the removal rate 0.13g/s and 0.121g/s consequently; sets with (2, 140, 4.88) and (4, 100, 2.22) provide the removal rate 0.087g/s and 0.079g/s consequently. Using the data presented on Fig. 5 it is possible to find other sets which provides such an effect with deviations no more than 15%. Unfortunately, we do not have enough experimental data to build dependencies similar to what we presented on Fig. 6.

The considered examples of geometrical and physical scalabilities are based on the available and presented here experimental data (Passive Catalytic Hydrogen Recombiner 2004, 2005). Because of some inherent uncertainty of experimental data, it would be quite supportive to consider this phenomenon, using modern numerical approaches like CFD calculations with taking into account the chemical kinetics of the catalytic recombination.

### Validation of the multistep mechanism within STAR CCM+

In this study, chemical kinetics of the catalytic recombination of hydrogen was analyzed with the use of the CHEMKIN format (Kee et al. 2000), the database of which is part of STAR CCM+ software (CD-Adapco 2017). The self-consistent problem of thermohydraulics and chemical kinetics can be successfully verified and solved using this software in a way it was fulfilled in (Reinecke et al. 2013, Baggemann et al. 2017, Malakhov et al. 2020).

Here we have used a detailed chemical reaction mechanism (the multistep reaction model) for the hydrogen oxidation on the catalyst surface. The surface kinetic model and associated rate expressions are largely based on previous work on oxidation reactions over Pt (Appel et al. 2002). We verified our approach using experimental data both for the AREVA type catalyst (rectangular sheets, REKO-3, Reinecke et al. 2005, Reinecke et al. 2010) and the RVK type catalyst (cylindrical rods, HYSAs, Malakhov et al. 2020).

### AREVA catalyst design

The catalyst sheets (stainless steel coated with washcoat/platinum catalyst material) are arranged in parallel forming vertical rectangular flow channels. Such a set-up represents a box-type recombiner section of AREVA, Reinecke et al. 2005 design (see Fig. 2).

The experimental setup of the REKO-3 facility contains only 4 catalyst sheets. Here we used a 2D approach in a way it was done in Reinecke et al. 2005, Rozeń 2015b, to verify our model based on using STAR CCM+ code. But we used all 4 sheets in our calculations with symmetry or external walls boundary conditions. Fig. 7 shows the experimental temperature profiles and our calculations for different hydrogen inlet concentrations at  $v=0.8$  m/s flow rate for air-hydrogen mixture. Fig. 8 shows the experimental hydrogen concentration profiles and our calculations for different inlet flow rates for air-hydrogen mixture. Both calculated temperature and hydrogen concentration profiles are demonstrated for the central channel. We have found a very reasonable agreement with the experimental data except the results for a very low concentration 0.5vol%. Here it has to be pointed out that the calculations are quite sensitive to the geometry details here. For example, the slight change of the distance between two plates (around 1mm) may change the temperature profiles by tens of degrees. We presume that such a sensitivity has to be taken into account in the processing of the experimental data as well.

**RVK catalysts design**

In order to verify our approach on the RVK type catalyst we use some experimental data reported in Malakhov et al. 2020 where the details of the experiments are discussed in detail. The flow channel (Fig. 8) is constructed as a vertical rectangular box (cross-sectional area 45.5 mm × 242 mm). The experimental setup allows one to investigate catalyst samples inside a vertical flow channel under well-defined conditions such as flow rate, and inlet concentration of hydrogen and air. The catalysts are cylindrical ceramic rods (height 64 mm, diameter 5 mm). The fourteen catalyst cylinders, coated with Pt catalyst, are arranged in parallel; they are held upright by a stainless steel frame. The temperatures of surfaces were measured with the use of the infrared camera (see Malakhov et al. 2020 for details).

In order to calculate the hydrogen concentration, sensors were fixed in two places (Fig. 9). The first sensor is installed in the centre, at the bottom of the

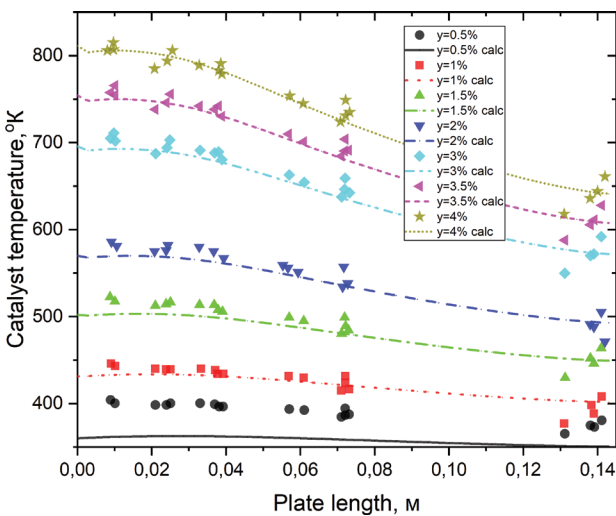


**Figure 7.** Temperature profiles: experimental data REKO-3 (Reinecke et al. 2005) and STAR CCM+ results

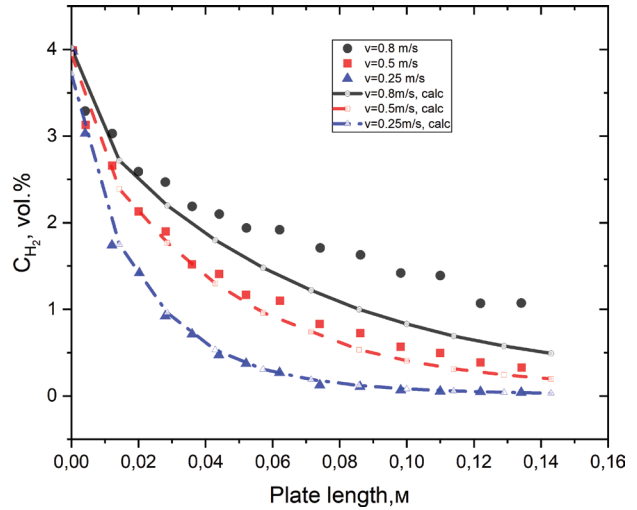


**Figure 8.** Hydrogen concentration profiles: experimental data REKO-3 (Reinecke et al. 2005) and STAR CCM+ results

catalyst, to determine the inlet hydrogen concentration. The second sensor is installed above the catalyst section, to determine the outlet hydrogen concentration after the catalytic reaction.

In this work, to verify our approach, we have used the data when the hydrogen concentration at the inlet is 4%, and the total mass flow rate of the gas mixture is 35 grams per minute. The rest of the experimental data can be found in Malakhov et al. 2020 and in our future works.

Fig. 10 shows the experimental temperature profiles for all the 14 rods and our calculations for the 7 rods on one side of the flow channel as our numerical model is symmetrical with respect to the plane between the 7<sup>th</sup> and 8<sup>th</sup> rods. But the experimental data do not show a com-

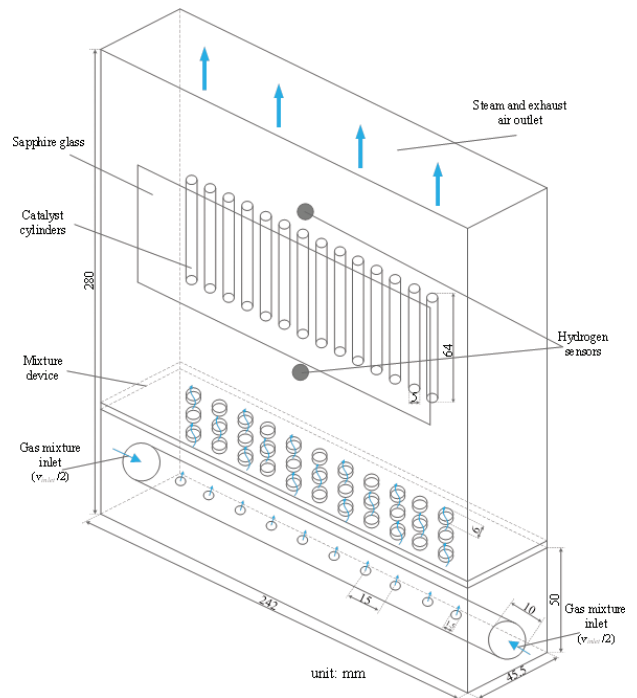


**Figure 9.** Experimental setup, it includes a catalyst section, hydrogen sensors, and gas flow controllers [taken from Malakhov et al. 2020).

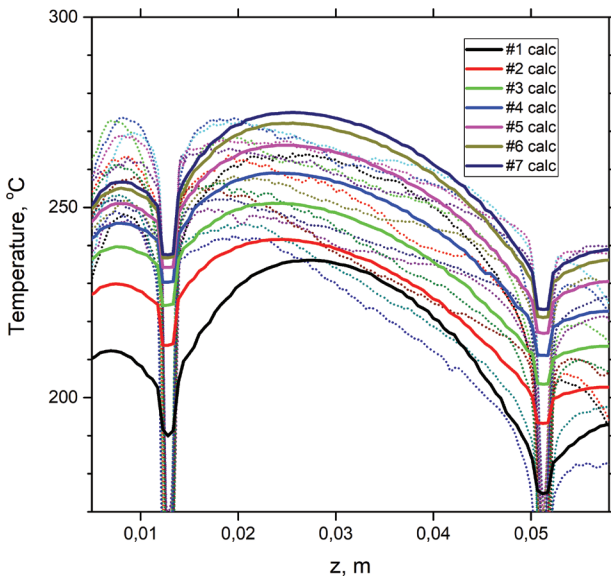


**Figure 10.** Temperature profiles: experimental data HYSA (Malakhov et al. 2020) (dotted curves) and STAR CCM+ results (solid curves)

plete symmetry in temperature profiles for symmetrically located rods. The detailed discussion of such a small discrepancy will be discussed elsewhere.

All temperature profiles shown in Fig. 10 have two minima. These minima correspond to the position of the parts of the stainless steel frames that hold the rods upright (Fig. 1, rods in the frame). Obviously, these steel elements affect the temperatures of the catalytic surface of the rods at their location (the rods are not held tightly by the frame and have a slight backlash). And the actual temperatures themselves in the area of the elements of the steel frame are the temperatures of the steel, not the catalytic surface of the rod. From the point of view of calculations, this introduces additional difficulties in the accuracy of modeling and especially in the accuracy of reproducing the experimental results in the vicinity of the frame elements. The comparison of the experimental results and the calculations show that the greatest differences are manifested precisely at the ends of the outermost rods in the frame. But on the whole, the applied model is in a good agreement with experimental data for such a complex geometry.

The experimental value of the hydrogen concentration at the point where the sensor is located above the rods is 1.82 vol.%, The calculated value is 1.58 vol.%, which can also be noted as quite acceptable accuracy.

Thus, we have checked the applicability of the multi-step hydrogen recombination mechanism on the available experimental data for both the AREVA plate recombiner and the RVK-type rod recombiner, and in the future, this approach can be used to construct a CFD model of the recombiner and test the scalability.

### Scalability with RVK type cylindrical catalysts

Since the catalytic unit of the recombiner consists of a large number of geometrically identical objects, in most cases there is no need to calculate its characteristics with

all tens of catalytic plates or hundreds of rods. It is enough to do it and verify it for the minimal possible geometry – the selected unit cell, as, for example, it was done for the verification of the REKO-3 experiments Reinecke et al. 2005 with catalytic plates. Naturally, the selected unit cell should reflect the symmetry of the arrangement of the rods in the catalytic block, and a separate analysis should be performed for edge cells that are close to the walls.

We have done some demo calculations to test geometric scalability. The calculations were performed for flow regimes with an initial temperature of 300 K, an initial hydrogen concentration of 4 vol.%, an initial velocity of a hydrogen-air mixture of 0.8 m/s, and an initial hydrogen concentration of 8%, an initial velocity of 3 m/s. A square packing of rods was considered. The radius of the catalyst rod is  $R = 0.0025$  m, height = 64 mm, the distance between the centers of the rods is  $d = 12.5$  mm, the distance between the centers of the rods and the walls is  $d = 12.5$  mm (for the variant where the effect of the wall of the recombiner box is taken into account). The simplest cell of a square packing, a symmetric cell, contains four quarters of rods (Fig. 11), a “2 \* 2” cell. The next in difficulty, “3 \* 3” cell contains 4 quarters, four halves and one whole rod (Fig. 11) and so on. Cells similar in construction are also considered near the wall of the catalytic block (Fig. 12).

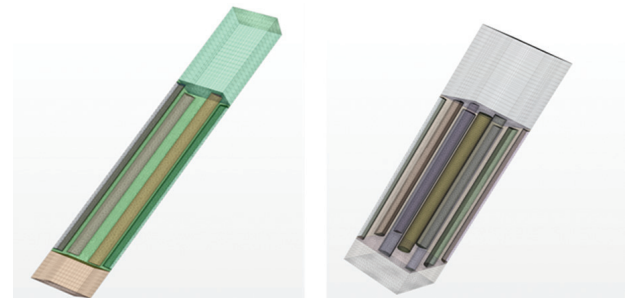


**Figure 11.** Symmetrical unit cell with quarters of four catalytic rods, “2\*2” case (left panel). Symmetrical unit cell with quarters of four catalytic rods, halves of four rods and one whole rod in the center, “3\*3” case (right panel).

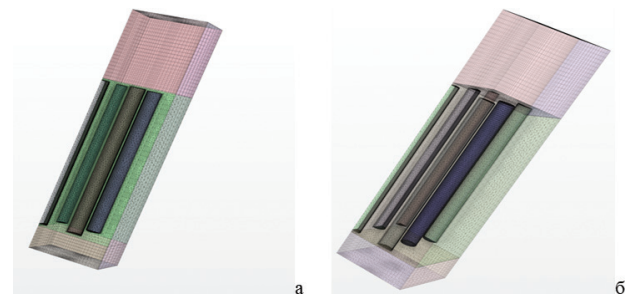


**Figure 12.** Symmetrical near the wall unit cell with quarters of two catalytic rods and halves of two whole rods near the wall, “nw 2\*2” case (left panel). Symmetrical unit cell with quarters of two catalytic rods, halves of three rods and one whole rod near the wall, “nw 2\*3” case (right panel).

Figs 13, 14 show the calculation results and their comparison for cells of similar symmetry, but different sizes. Obviously, increasing the scale, that is, the geometric size, does not lead to a change in the density (concentra-

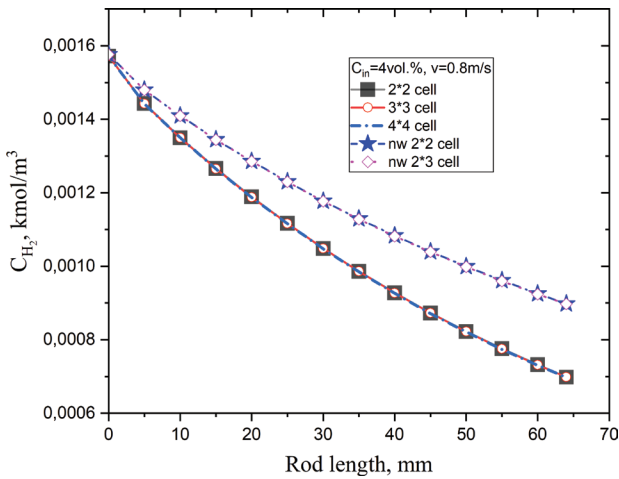


**Figure 13.** The hydrogen molar density along the rods in different cells

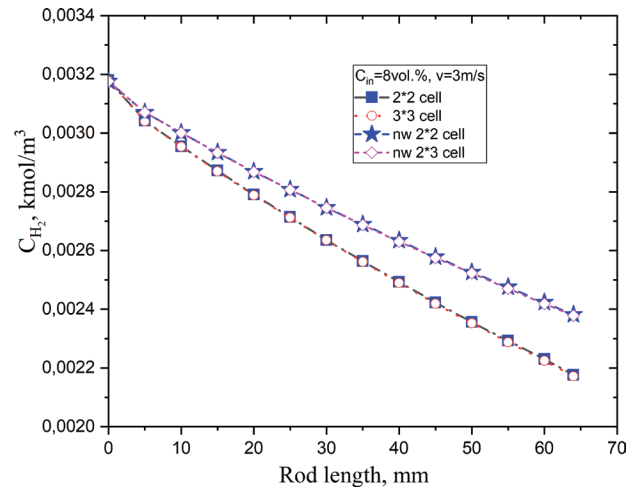


**Figure 14.** The hydrogen molar density along the rods in different cells

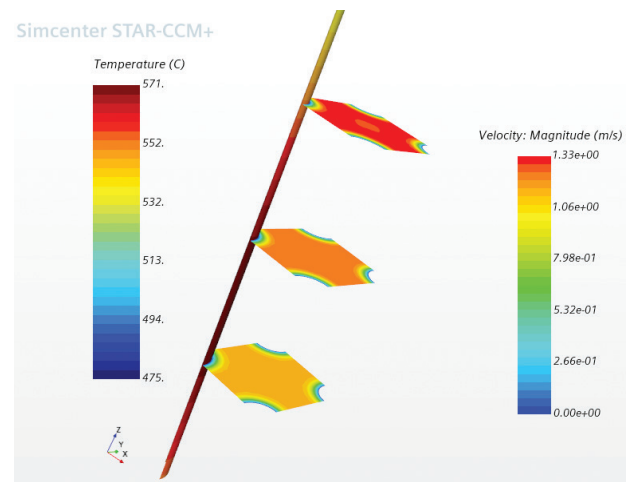
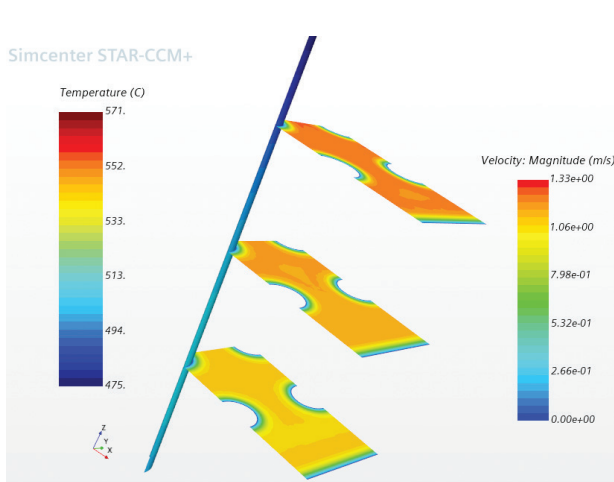


**Figure 15.** Temperatures on the surface of the rod and the distribution of velocities in some sections for the cell “2 \* 2”(left panel) and for the cell “nw 2 \* 2”(right panel). Initial hydrogen concentration is 4vol.%, initial mixture velocity is 0.8 m/s

tion) of hydrogen in similar cells, and the selected initial velocity and geometry do not affect this. Thus, if we consider the recombiner as consisting of identical symmetric cells, then there is no need to carry out laborious calculations taking into account all catalytic elements (rods in this case), and the hydrogen removal rate can be calculated based on only one cell. The general operation of the recombiner can then be used according to the scheme proposed in Reinecke et al. 2005. On the other hand, if the recombiner is not large enough, then the effect of edges (Fig. 12) may be noticeable. Figs 13, 14 show the calculations of the hydrogen concentration for some edge cells, “nw 2 \* 2” and “nw 2 \* 3”. As one can see, the hydrogen concentration at the outlet for these cells is 15–20% higher than for the considered symmetric cells. That is, the hydrogen removal rate of these cells is lower by this value. This also manifests itself in lower rod surface temperatures and a lower rate of exit of the gas mixture from the edge cell (Fig. 15). For the case considered in Fig. 15, it can be seen that the maximum temperature of the rod in the edge cell is 50–60 °C lower than in a conventional cell, and the gas mixture exit rate is 10–15% lower. Thus, knowing the ratio of the total number of symmetric and

edge cells, it is possible to estimate the necessary corrections for the performance of the entire recombiner, as well as the corrections for the average values of characteristics such as velocity, temperature, density, and pressure. The need for such corrections is determined by the formulation and goals of specific calculations. It is quite clear from general considerations and the above calculations that such edge effects can be neglected for large recombiners.

Another interesting feature of scaling is the scaling, which we call physical. Namely, for a given volumetric hydrogen concentration and the same inlet temperature to pressure ratios, which corresponds to the same initial hydrogen density, the density distribution is maintained throughout the cell (Fig. 16). Calculations are made for the cell “2 \* 2”, the initial hydrogen concentration is 4%, the initial velocity is 0.8 m/s. Small discrepancies are most likely related to the accuracy of the calculations and are a numerical error. Subsequently, this effect will be tested on more complex large geometries. But the calculations show that this type of scaling follows from the assumption that all gases in the mixture are ideal and that there is no condensation. Most likely, there are other types of scalabilities associated with the initial velocity of the hydrogen-air mixture.

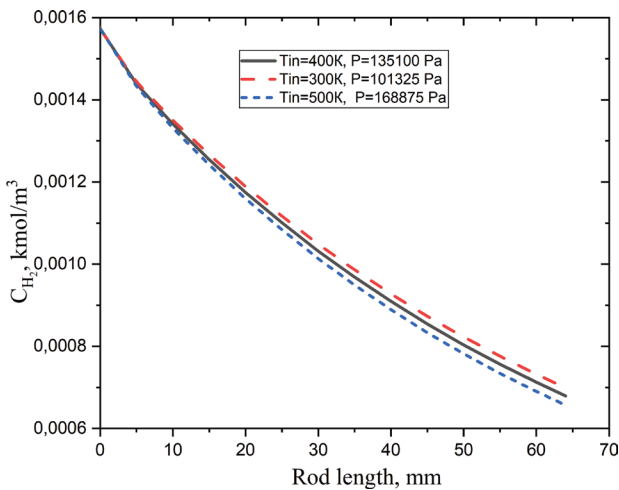


**Figure 16.** The hydrogen molar density along the rods for different temperatures and pressures

## Conclusion

In this study it was shown that regardless of the type of geometry of the catalytic elements in a recombiner, and to the main extent, the hydrogen removal rate is determined by the area of the catalytic surface and the molar

density of hydrogen at the inlet. Here we only considered the cases with oxygen excess conditions. We presume that oxygen deficiency cases as well as the presence of carbon monoxide and steam should not change the effects of scalability. But it will be studied elsewhere.

We analyzed the existing empirical dependencies for hydrogen removal rates of two types of recombiners and fulfilled a number of CFD calculations using the STAR CCM + code.

An essential part of the approach is the use of a detailed chemical reaction mechanism (the multistep reaction model) for the hydrogen oxidation on the catalysts surface. This approach possesses more universality for determining the hydrogen removal rate both under natural circulation conditions and under conditions of forced circulation in the area of the location of recombiners, which is clearly necessary for the numerical justification of severe accidents with hydrogen release.

Numerical examples were used to demonstrate the geometric and physical scalability of the functioning of the catalytic elements, which can be and will be used to construct an advanced CFD model of the recombiner and its more numerically realizable interaction with the hydrogen-air environment in emergency modes.

## References

- Appel C, Mantzaras J, Schaeren R, Bombach R, Inauen A, Kaeppli B, Bernd Hemmerling B, Stampanoni A (2002) An Experimental and Numerical Investigation of Homogeneous Ignition in Catalytically Stabilized Combustion of Hydrogen/Air Mixtures over Platinum. *Combustion and Flame* 28(4): 340–368. [https://doi.org/10.1016/S0010-2180\(01\)00363-7](https://doi.org/10.1016/S0010-2180(01)00363-7)
- Arnould F, Bachelier E, Auglaire M, De Boeck B, Braillard O, Eckardt B, Ferroni F, Moffett R, Van Goethem G (2021) State of the art on hydrogen passive autocatalytic recombiner. NCL collection store, 1–23. [https://inis.iaea.org/collection/NCLCollectionStore/\\_Public/33/020/33020098.pdf](https://inis.iaea.org/collection/NCLCollectionStore/_Public/33/020/33020098.pdf)
- Avdeenkov AV, Sergeev VV, Stepanov AV, Malakhov AA, Koshmanov DY, Soloviev SL, Bessarabov DG (2018) Math Hydrogen Catalytic Recombiner: Engineering Model for Dynamic Full-Scale Calculations. *International Journal of Hydrogen Energy* 43(52): 23523–23537. <https://doi.org/10.1016/j.ijhydene.2018.10.212>
- Bachelier E, Arnould F, Auglaire M, de Boeck B, Braillard O, Eckardt B, Ferroni F, Moffett R (2003) Generic approach for designing and implementing a passive autocatalytic recombiner PAR-system in nuclear power plant containments. *Nuclear Engineering and Design* 221: 151–165. [https://doi.org/10.1016/S0029-5493\(02\)00330-8](https://doi.org/10.1016/S0029-5493(02)00330-8)
- Baggemann J, Jahn W, Kelm S, Reinecke E-A, Allelein H-J (2017) Numerical Study on the Influence of Different Boundary Conditions on the Efficiency of Hydrogen Recombiners inside a Car Garage. *International Journal of Hydrogen Energy* 42(11): 7608–7616. <https://doi.org/10.1016/j.ijhydene.2016.04.084>
- Blanchat TK, Malliakos A (1999) Analysis of hydrogen depletion using a scaled passive autocatalytic recombiner. *Nuclear Engineering and Design* 187: 229–239. [https://doi.org/10.1016/S0029-5493\(98\)00283-0](https://doi.org/10.1016/S0029-5493(98)00283-0)
- CD-Adapco S (2017) Star CCM+ User Guide Version 12.04. CD-Adapco. New York (USA).
- Della Loggia E (1992) Hydrogen behaviour and mitigation in water-cooled nuclear power reactors (No. EUR--14039), CEC.
- Ferroni F, Schiel L, Collins P (1994) “Containment Protection with Hydrogen Recombiners”. *Atw. Atomwirtschaft, Atomtechnik* 39(7): 513–514.
- Framatome (2022) Hydrogen Control System: mixers, igniters, recombiners. <https://www.framatome.com/solutions-portfolio/portfolio/product?product=A0640>
- International Atomic Energy Agency (2001) Mitigation of Hydrogen Hazards in Severe Accidents in Nuclear Power Plants. IAEA (2011), Mitigation of hydrogen hazards in water cooled power reactors. IAEA-TEKDOC-1196.
- Jae-Won P, Byung-Ryung K, Kune YS (2011) Demonstrative testing of honeycomb passive autocatalytic recombiner for nuclear power plant. *Nuclear Engineering and Design* 241: 4280–4288. <https://doi.org/10.1016/j.nucengdes.2011.07.040>
- Kee RJ, Rupley FM, Miller JA, Coltrin ME, Gracar JF, Meeks E, Moffat HK, Lutz AE, Dixon-Lewis G, Smooke MD, Warnatz J, Evans GH, Larson RS, Mitchell RE, Petzold LR, Reynolds WC, Caracotsios M, Stewart WE, Glarborg P, Wang C, Adigun O (2000) CHEMKIN Collection, Release 3.6, Reaction Design, Inc., San Diego, CA.
- Klauk M, Reinecke E-A, Kelm S, Meynet N, Bentaib A, Allelein H-J (2014) Passive auto-catalytic recombiners operation in the presence of hydrogen and carbon monoxide: Experimental study and model development. *Nuclear Engineering and Design* 266: 137–147. <https://doi.org/10.1016/j.nucengdes.2013.10.021>

- Malakhov AA, du Toit MH, du Preez SP, Avdeenkov AV, Bessarabov DG (2020) Temperature Profile Mapping Over a Catalytic Unit of a Hydrogen Passive Autocatalytic Recombiner: Experimental and CFD study. *Energy Fuels* 34(9): 11637–11649.
- Mayer L, Blanchat TK, Pilch M (2009) Direct Containment Heating Experiments at Low Reactor Coolant System Pressure in the Surtsey Test Facility, NUREG/CR-5746.
- Passive Catalytic Hydrogen Recombiner (2004) RVK-500 (Passivnyi kataliticheskii recombimator vodoroda RVK-500). *Tekhnicheskie usloviya RET-101.00.000*. [in Russian]
- Passive Catalytic Hydrogen Recombiner (2005) RVK-500, RVK-1000 (Passivnyi kataliticheskii recombimator vodoroda RVK-500, RVK-1000). *Tekhnicheskie usloviya RET-101.00.000*. [in Russian]
- Reinecke E-A, Bentaib A, Kelm S, Jahn W, Meynet N, Caroli C (2010) Open Issues in the Applicability of Recombiner Experiments and Modelling to Reactor Simulations. *Progress in Nuclear Energy* 52(1): 136–147. <https://doi.org/10.1016/j.pnucene.2009.09.010>
- Reinecke EA, Boehm J, Drinovac P, Struth S, Tragsdorf IM (2005) Modelling of catalytic recombiners: Comparison of REKO-DIREKT calculations with REKO-3 experiments. *Proceedings of the International Conference “Nuclear Energy for New Europe 2005”*. Bled, Slovenia, September 5–8, 2005, 092.1–092.10.
- Reinecke E-A, Kelm S, Jahn W, Jäkel C, Allelein H-J (2013) Simulation of the Efficiency of Hydrogen Recombiners as Safety Devices. *International Journal of Hydrogen Energy* 38(19): 8117–8124. <https://doi.org/10.1016/j.ijhydene.2012.09.093>
- Rozeń A (2015a) A mechanistic model of a passive autocatalytic hydrogen recombiner. *Chemical and Process Engineering* 36(1): 3–19. <https://doi.org/10.1515/cpe-2015-0001>
- Rozeń A (2015b) Modelling of a passive autocatalytic hydrogen recombiner – a parametric study. *Nukleonika* 60(1): 161–169. <https://doi.org/10.1515/nuka-2015-0002>
- Russkiye Energeticheskiye Tekhnologii (2021) Passive catalytic hydrogen recombiners [Пассивные каталитические рекомбинаторы водорода]. <https://retech.ru/pkrv>
- Saint-Just J, Etemad S (2016) 10 - Catalytic combustion of hydrogen for heat production. In: *Compendium of Hydrogen Energy*; Elsevier Ltd., Fairfield, 263–287. <https://doi.org/10.1016/B978-1-78242-363-8.00010-4>
- Tarasov OV, Kiselev AE, Filippov AS, Yudina TA, Grigoruk DG, Koshmanov DE, Keller VD, Khristenko EB (2017) Development and Verification of a Model of RVK-500, -1000 Recombiners for Modeling the Containment Shells of NPP with VVER by Computational Hydrodynamics. *Atomic Energy* 121(3): 131–136. <https://doi.org/10.1007/s10512-017-0178-3>